Available online at www.sciencedirect.com
SCIENCE DIRECT®
Journal of Catalysis 237 (2006) 49–57
JOURNAL OF CATALYSIS
www.elsevier.com/locate/jcat

A versatile and compact experimental apparatus for the on-line spectroscopic study of liquid-phase heterogeneous catalytic systems

Feng Gao, Kim Poi Ng, Chuanzhao Li, Karl I. Krummel, Ayman D. Allian, Marc Garland *

Department of Chemical and Biomolecular Engineering, 4 Engineering Drive 4, National University of Singapore, Singapore 117576

Received 16 July 2005; revised 12 September 2005; accepted 13 September 2005

Available online 17 November 2005

Abstract

A versatile and compact experimental system is described for the study of fine-chemistry liquid-phase heterogeneous catalysis. The general experimental system consists of a stirred tank (25–100 mL), pump, tubular reactor, spectrometer(s), and injection block for liquid-phase perturbations, all in a closed-recycling configuration. The basic designs of the in-house-constructed components are provided. The system was characterized with respect to gas–liquid mass transfer, mixing, liquid–solid mass transfer, and intraparticle diffusion. The utility of the system is demonstrated with a heterogeneous catalytic reaction—the racemic hydrogenation of acetophenone over Pt/Al_2O_3—using on-line Fourier transform infrared (FTIR) analytics. Liquid–solid mass transfer and intraparticle diffusion were studied by varying the liquid hourly space velocity (LHSV) as well as the catalyst particle sizes used. The reaction rates based on the instantaneous reagent concentrations were precisely evaluated using on-line FTIR measurements. The rather novel inclusion of an injection/sampling block was particularly useful for performing multiple perturbations of reagents, a situation neither normally available nor convenient for the experimentalist, thus facilitating outstanding spectral deconvolution using band-target entropy minimization. The small total liquid-phase volume involved (≈15 ml) would facilitate the frugal use of chiral reagents/auxiliaries as well as isotopically labeled components.

Keywords: Recycle reactor; Liquid-phase catalysis; On-line FTIR spectroscopy; Multiple perturbations

1. Introduction

In the chemical sciences, the use of on-line or even in situ spectroscopic measurements, in contrast to off-line and ex situ measurements, is becoming more common. Indeed, the advantages of this approach can be great. This is already quite evident in the field of homogeneous catalysis, where in situ spectroscopic measurements under industrially relevant reaction conditions are becoming rather common [1]. Instantaneous concentrations of both intermediates and reagents can be measured, exact turnover frequencies can be obtained, and a detailed mechanistic understanding can be achieved [2]. In heterogeneous catalysis, in situ spectroscopic characterization of the solid catalysts under industrially relevant reaction conditions is usually restricted to extended X-ray absorption fine structure/X-ray absorption near edge structure [3,4], Mössbauer spectroscopy [5], Fourier transform infrared (FTIR)/diffuse reflectance infrared Fourier transform (DRIFT) spectroscopy [6–8], Raman spectroscopy [9], ultraviolet–visible (UV–vis) diffuse reflectance spectroscopy [10], and magic angle spinning–nuclear magnetic resonance [11]. On-line spectroscopic measurement of the associated fluid phase to determine the products and accurate kinetics has received considerably less attention. Because most heterogeneous catalytic fine-chemical syntheses are conducted in a liquid phase as a solid–liquid suspension (slurry) or occasionally in a packed bed, there exists considerable opportunities to combine various types of technical know how to achieve useful on-line spectroscopic measurements of the fluid-phase alone.

There are some important hardware considerations for on-line spectroscopic studies of liquid-phase fine-chemical heterogeneous catalytic systems. First, the experimental system benefits from a recycle configuration, to minimize the quantities of chemicals used. Second, both packed-bed and gas–liquid stirred tank are needed for maximum experimental flexibility.

* Corresponding author.
E-mail address: chemvg@nus.edu.sg (M. Garland).

0021-9517/$ – see front matter
doi:10.1016/j.jcat.2005.09.031

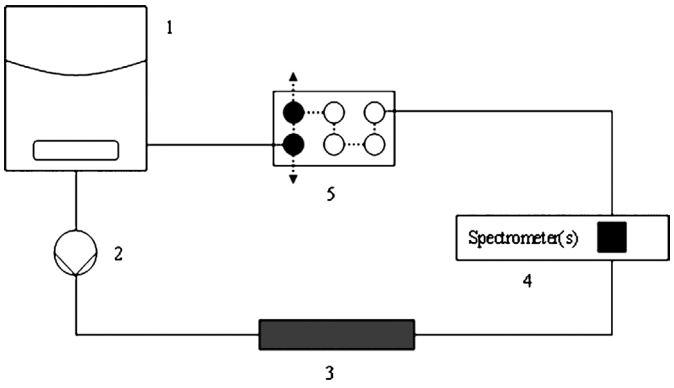

Fig. 1. General schematic diagram of a recycle system applicable to small-volume fine-chemical heterogeneous catalytic liquid-phase reactions. Components: (1) stirred tank, (2) pump, (3) packed bed, (4) spectrometer(s), (5) injection/sampling block (open symbols are six-way HPLC injection valves, closed symbols are six-way HPLC sampling valves).

The stirred tank provides a gas buffer in the event that a gaseous reagent is used. Third, the system must have a device for reliably changing/perturbing the fluid compositions during the course of the experimental run. Such a device could be a series of high performance liquid chromatography (HPLC) rotary valves. A schematic diagram of such an experimental system, including a pump for recirculation and a spectroscopic cell, is shown in Fig. 1.

The use of a general experimental system such as that shown in Fig. 1 for reliable kinetic studies entails a number of considerations. These include characterization of the system in the absence of reaction, that is, (i) gas–liquid mass transfer for the stirred tank and (ii) mixing and recycle residence time distribution in the entire system, as well as characterization of the system in the presence of reaction to confirm (iii) negligible liquid–solid transport resistance, (iv) negligible intraparticle diffusion resistance, and (v) differential conversion over the packed bed. The latter is important to provide complete uniformity of concentration and temperature throughout the catalyst bed [12].

Perhaps most important, classical methods of off-line analysis are intrinsically ill suited for system identification. On-line measurements are far more appropriate than sampling [13]. The general experimental setup shown in Fig. 1 allows not only on-line FTIR measurements, but also a few nonobvious opportunities for system identification. First, because of the convenient multiple-valve injection/sampling block, the system can be readily used in semibatch mode (even under high internal pressures), allowing very extensive experimental designs and resulting in coverage of a very wide range of reaction conditions in a single run [14]. Second, extensive experimental designs consisting of multiple perturbations permit the application of very advanced signal deconvolution programs, like band-target entropy minimization (BTEM), to the very large sets of spectroscopic data [15–17]. The injection/sampling block shown in Fig. 1 was designed to facilitate such multiple perturbations and meet the prerequisites for successful deconvolution. Finally, the aforementioned two issues combined can facilitate the rapid and reliable determination of the algebraic structure of the catalytic network [18], and then the detailed kinetics [19], at least in homogeneous catalytic systems.

Briefly, it should be noted that BTEM is essentially a soft-modeling approach to obtaining the pure component spectra of species without any a priori information. The experimentalist does not need to know or estimate the number of species present in advance. Moreover, no presuppositions are needed concerning the particular type of spectral characteristics present, that is, whether the spectral bands follow a Lorentzian, Gaussian, Pearson, or other distribution. It is recognized that copious spectroscopic data, obtained from a large number of perturbations, helps to untangle spectroscopic signals, because spectral co-linearities are more readily avoided and greater signal variation can be obtained. Thus BTEM has been repeatedly used to identify new and nonisolatable species and transient intermediates.

In the present contribution, an experimental system similar to Fig. 1 is presented, including details of the components designed and constructed in-house and its tests for on-line heterogeneous catalytic spectroscopic measurements of the fluid phase. The selected reaction is the racemic hydrogenation of acetophenone over Pt/Al_2O_3. This reaction was selected because hydrogenation—specifically, enantioselective hydrogenation—is a topic of constant academic interest and considerable economic importance to the agrochemical, fine-chemical, and pharmaceutical industries [20]. Although the present example of racemic hydrogenation of acetophenone over Pt/Al_2O_3 is not stereo-specific, it does allude to its modified form and hence to the intensely studied Orito reaction [21–27] and extensions to more sophisticated on-line/off-line spectroscopies, including circular dichroism measurements [28]. Finally, by keeping the experimental system simple and hence cost-effective, the experimentalist is able to reserve entire setups for different catalytic systems, thereby avoiding the problem of cross-contamination between catalytic experiments.

2. Experimental

2.1. General issues

The catalyst used in this study is a commercial product, Engelhard 4759 (5% Pt/Al_2O_3), with the following catalyst properties: mean particle size, 55 μm; BET, 140 m^2/g; mean pore radius, 50 Å; real density, 5.0 g/mL; platinum loading, 4.65%; platinum dispersion, 0.28; apparent density, 1.9 g/mL. The catalyst was pretreated in a fixed-bed reactor by flushing with 3–4 L/h N_2 (99.9%) at room temperature for 10 h, followed by a reduction treatment in H_2 at 400 °C for 120 min. After cooling to room temperature in H_2, the catalyst was immediately transferred to a Schlenk tube and kept under argon.

Toluene (Mallinckrodt; 99.9%) was distilled from sodium–potassium alloy under purified argon for around 5 h to remove the trace water and oxygen. Acetophenone (Aceph; Aldrich, 99%) and 1-phenylethanol (Phel; Acros organics, 98%) were mixed and shaken with anhydrous 4 Å molecular sieves to remove trace water and oxygen.

Standard Schlenk techniques were used in the experiments. All solution preparations and transfers were carried out under purified argon (99.9995%; Saxol; Singapore) atmosphere. The argon was further purified before use by passing it though a deoxy and zeolite column before use to adsorb trace oxygen and water. Purified hydrogen (99.9995, Saxol) was also further purified through a deoxy and zeolite column before being used in hydrogenation. The pressure of the hydrogen was kept almost constant during the reaction time, because a 1-L reservoir was connected to the 25-mL system. The literature data for the solubility of hydrogen in anhydrous toluene at 298.15 K as a function of total pressure were used to calculate the dissolved hydrogen concentration [29]. Weights were measured with a precision of 0.001 g; volumes, with a precision of 0.05 mL.

2.2. Experimental procedure

The following is a typical experimental procedure. First, the catalyst was prepacked in a 2.1-mm (diameter) × 50-mm (length) HPLC cartridge. The rest of the reactor volume was filled with inert quartz sand. Then the whole system was vacuumed before 15 mL toluene was transferred under argon to the stirred tank. After that, the whole system was briefly vacuumed again before the required hydrogen partial pressure was added to the stirred tank. The stirrer was then started first to saturate the solvent with hydrogen. The controlling needle valves were subsequently opened, and the high-pressure metering pump was started. The stirring speed was set at 400 rpm, and the flow rate was set to 3–7 mL/min. Circulation of the solvent lasted done for ca. 15 min to ensure saturation of hydrogen in the recycling system and thermal equilibration of the apparatus. At time $t = 0$ min, a program was executed to record the spectra every minute. Then, at a predetermined time, a certain amount of reagent was injected through one of the HPLC valves. At this point, the hydrogenation runs were initiated.

The reactor was immersed in a water bath (Polyscience 9505) at 0 °C. The variation in temperature was ca. ±0.5 °C.

2.3. Spectroscopic issues

Experimental on-line spectra contain signals not only from the solution in the system, but also from the cell, gas-phase components in the spectrometer, and so on. Quantitative analysis requires pure component spectra, either from appropriate references or from some robust self-modeling curve resolution (SMRC) program. In the present study, a combination of preconditioned reference spectra and pure component spectra obtained from BTEM were used.

2.3.1. On-line precatalytic spectra and spectral analysis

One set of perturbations of Aceph was carried out, in the absence of catalyst and hydrogen, to obtain pure component spectra before the catalytic reaction runs. Inert helium, not hydrogen, was used as the buffer gas on the system. Circulation speed was ca. 2 mL/min. The scanning range was 1000–4000 cm^{-1}, and 130 spectra were acquired. Visual inspection

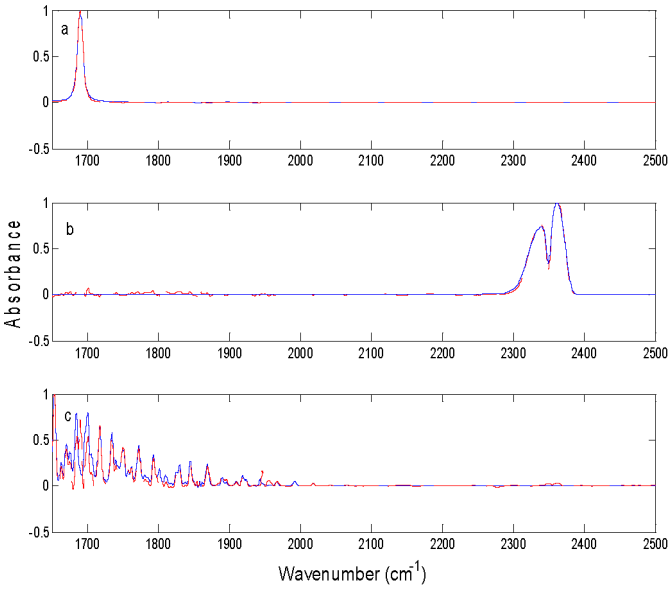

Fig. 2. The experimental references and BTEM estimates for Aceph, carbon dioxide and moisture in the region of 1650–2500/cm. Solid lines are experimental references; dashed lines are BTEM estimates; (a) acetophenone; (b) carbon dioxide; (c) moisture.

of on-line spectra found high transmission of solvent and background in the 1650–2500 cm^{-1} region, and thus this region was selected for spectral analysis.

The pure component spectrum of toluene in a CaF_2 cell was obtained by entropy minimization spectral subtraction [30]. Other major component spectra were deconvoluted via the application of BTEM. The procedures for the deconvolution were as follows. Singular value decomposition was used to decompose the raw experimental semibatch absorbance data matrix with 130 spectra and 4251 channels. The resulting right singular vectors of the V^T matrix were visually inspected. Three extrema (wavenumbers ca. 1690, 1717, and 2361 cm^{-1}) for significant spectral features were used as targets in the BTEM algorithm. Further details about BTEM have been published previously [15–17]. The resulting BTEM estimates and experimental pure component reference spectra for the major components Aceph, carbon dioxide, and moisture are plotted in Fig. 2. This figure shows that the spectral similarities of the estimates with the authentic references are very high, and spectral contributions from the cell and other sources have been effectively eliminated.

Calibrations showed that the molar absorptivity of acetophenone was 619.1 L/(mol cm). The Lambert–Beer law was then used to obtain concentrations from the reactive mid-infrared FTIR absorbance spectra [18].

It is noteworthy that such model-free and effective deconvolution is only possible when copious spectral data are recorded and when multiple perturbation experimental designs can be conveniently implemented. The present semibatch system for on-line spectroscopic measurements, equipped with a multiple-valve injection/sampling block, greatly facilitated the model-free deconvolution. Although the present example is rather simple, this general approach has been shown to apply to much more complex multicomponent systems as well.

2.3.2. On-line reaction spectra and spectral analysis

Typical on-line reaction FTIR spectra in the 1000–4000 cm^{-1} region were recorded every minute. At pressures of ca. 2 bar total pressure, and a flow rate of ca. 1 cm/s, very little addition noise was induced in the spectra during flow, despite the 0.37-mm optical path length used. In this study, the transmission of solvent and background in the 1650–1750 cm^{-1} region is high, and the characteristic peak of C=O of acetophenone has a strong signal at 1690 cm^{-1}. Because of the simple test reaction and chemistry involved, this region alone was used for quantitative analysis.

In a manner similar to the signal processing for the precatalytic spectra, the preconditioned reference spectrum of toluene in a CaF_2 cell and other major component spectra obtained from BTEM were used for quantitative analysis.

3. System design

The constructed recycling apparatus follows the layout shown in Fig. 1. The following commercial components were used for testing the assembled system: a metering pump (Eldex model B-100-S-2-CE) or a high-pressure hermetically sealed gear pump (Micropump model 445R), a packed bed fashioned from an empty HPLC cartridge (Agilent), and a Perkin–Elmer System 2000 FTIR spectrometer.

Three components required considerable design considerations: the stirred tank, the spectroscopic cell and the injection/sampling block. The primary mechanical issues in the design were (i) possible use at elevated pressures ($P = 1$–50 bar) and ca. room temperature ($T = 0$–$50\,^{\circ}C$), (ii) incorporation of integrated heat exchange manifolds, and (iii) ease of assembly/disassembly and reliable sealing of components. In what follows, we discuss rather detailed design considerations and present some designs.

3.1. Two-phase stirred tank

Adequate gas–liquid mass transfer and liquid-phase mixing were the primary transport considerations for the isothermal two-phase stirred tank. Normally, for well-designed tanks, a liquid height-to-tank diameter ratio of ca. $H/D \approx 1$ and a stirrer length-to-reactor diameter of ca. $d/D \approx 0.3$ would be used [31]. The total volume of the constructed stirred tank was ca. 24.5 mL (∅25 × 50 mm). The liquid-phase reaction volume in the stirred tank was ca. 11 mL (including the volume of the stirring bar, ca. 1 mL). Therefore, the height of the liquid in reactor satisfies the requirement of $H/D \approx 1$. Because magnetic stirring was used instead of a mechanical turbine, the $H/4$ position for the turbine position could not be satisfied. Accordingly, to compensate, the length of the magnetic stirrer was ca. 15 mm, twice the required $d/D \approx 0.3$. The stirrer diameter of 9 mm helped improve the gas–liquid mass transfer and liquid-phase mixing (vida infra).

The extra mechanical considerations for the stirred tank were integrated extra-high-field strength magnetic stirrers and two gas inlet/outlets, two liquid inlet/outlets, and 0.5-μm frits.

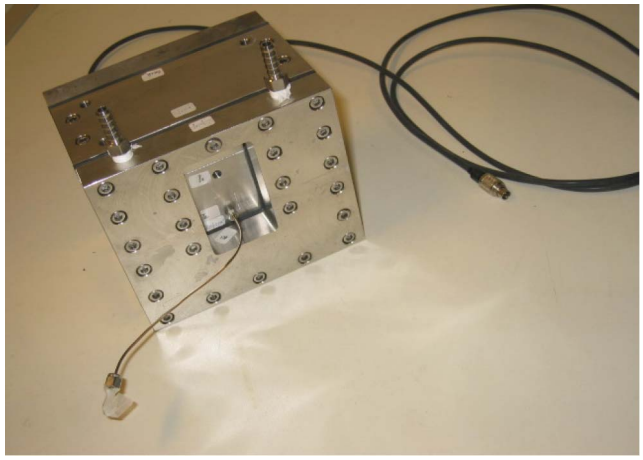

Fig. 3. A photograph of the compact stirred tank. View from front, showing heat exchange manifold with inlet/outlet for heat exchange fluid. Recess permits connections for (i) liquid inlet and (ii) gas inlet. Backside heat exchange manifold has recess which permits connections for (i) magnetic stirrer control cables, (ii) liquid outlet filter assembly, and (iii) gas outlet.

Accordingly, the stirred tank was designed from seven interconnected stainless steel plates. The five central plates with integrated heat exchange contained the stirred tank and magnetic stirrers; the last two exterior plates were the manifolds needed for the heat exchanger. The final dimensions of the 25-mL stirred tank were 14 × 10.5 × 12 cm. The compact stirred tank is shown in Fig. 3.

3.2. FTIR cell

Absence of dead volumes was the primary transport consideration. Dead volumes, particularly at and around the window areas and seals, are detrimental to both the residence time distribution tests as well as to the spectroscopy. The extra mechanical issues for FTIR cell were the mechanical integrity of the optical windows and the presence of two liquid inlet/outlets. Accordingly, the spectroscopic cell was designed from seven interconnected stainless steel plates. The five central plates with integrated heat exchange contained the spectroscopic windows, and the last two exterior plates were the manifolds needed for the heat exchanger. The final dimensions of the spectroscopic cell were ca. 14 × 10.5 × 12 cm. The compact cell is shown in Fig. 4.

3.3. Injection/sampling block

The injection/sampling block used four different-size HPLC six-port valves (Valco Instruments C1-2006; 2-, 20-, 100-, and 250-μL sampling loops) for injections and two same-size HPLC six-port valves (Valco Instruments C2-2006; 20-μL sampling loops) for sampling. The extra mechanical concerns were the connectivity of the six-port values used and the positions in the heat exchanger block. Accordingly, the injection/sampling block was designed from three interconnected aluminum plates. The six-port valves were inserted into the central aluminum block. The final dimensions of the injection/sampling block

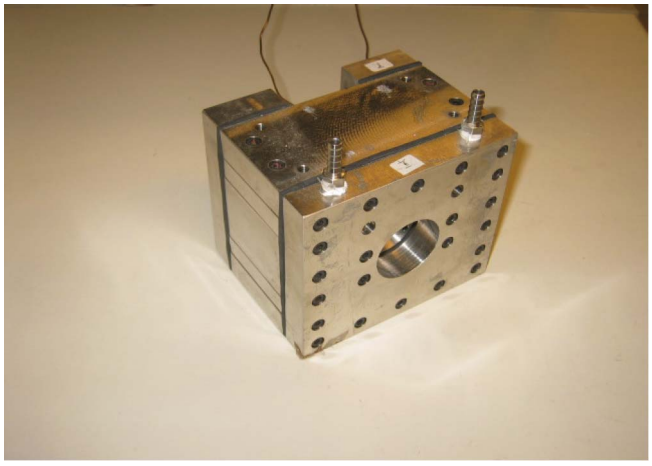

Fig. 4. A photograph of the compact cell. View from front, showing heat exchange manifold with inlet/outlet for heat exchange fluid. Recess for infrared beam is visible in photo as is part of window screw assembly. Stack of 5 central plates for (i) window assembly, (ii) exchange cross-flow, and (iii) reaction fluid inlet and outlet are visible from side. Backside heat exchange manifold has recesses which permit (i) exit of infrared beam and (ii) connection for reaction fluid inlet and outlet.

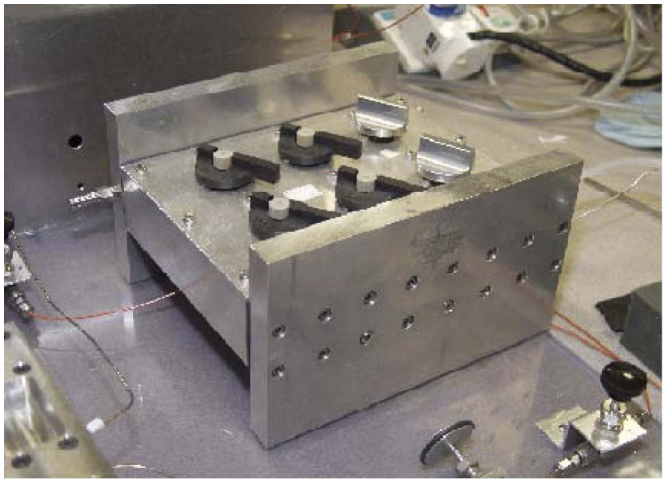

Fig. 5. A photograph of the compact injection/sampling block, with four six-way injection valves and two six-way sampling valves. Heat exchanger is present in central aluminum block. Front and back sides are heat exchange manifolds. Inlet for heat exchange fluid is visible on left. The two pieces of red PEEK tubing on left and right represents recycle transfer line for reaction fluid.

were ca. 22.6 × 21 × 14 cm. The compact injection/sampling block is shown in Fig. 5.

3.4. Isothermal control of reaction

The recycle line for the entire system was made of 1/16″ stainless steel or PEEK tubing. In a typical application at room temperature or above (i.e., using conventional organic synthesis or homogeneous catalysis), all system components and recycle tubing would be heat-traced so that the entire system is isothermal. However, in this particular specialized application, heterogeneous catalysis was conducted at $T = 0\,^{\circ}\mathrm{C}$. To keep the logistics simple, about 60 cm of this stainless steel tubing was used as a heat exchanger and immersed in a chiller along with the packed-bed reactor. Simple heat transfer calculations showed that this was more than enough length to cool the solution to $T = 0 + \delta\,^{\circ}\mathrm{C}$ at the flow rates used. The temperature variation along the catalyst bed was quite small, because the conversion of the substrate per pass was always <0.5%. The temperature of the fluid in other parts of the system, such as the pump, stirred tank, and FTIR cell, was held at room temperature.

3.5. Other equipment issues and supplementary material

The plates were easily and economically machined by a commercial machine shop. The most difficult commercial parts to obtain were the extra-high-field strength magnetic stirrers and the 40-mm-diameter × 15-mm-thick CaF_2 infrared windows. The stirrers (Variomag Micro P; H + P Labortechnik) were needed for stirring in the presence of 5-mm-thick stainless steel walls. With a Young's modulus of 11×10^6 psi, these CaF_2 optical windows (Korth Kristalle GMBH) were significantly overdesigned. Other window materials and other spectroscopies have also been used with these cells (e.g., quartz for UV–vis applications).

Supplementary material for this section includes (i) detailed mechanical drawings (CAD); (ii) additional photographs of all of the parts, as well as a partially assembled device; (iii) connectivity of the valves and tubing; (iv) and details for the consumables (i.e., Kalrez O-rings, frits, nuts, etc.).

4. System characterization

The complete connected system is illustrated in Fig. 1. The typical liquid volume in the stirred tank was 11 mL (including the volume of the stirring bar, ca. 1 mL). This resulted in an operating H/D ratio of ca. 1. The typical liquid volume of the entire recycle loop, consisting of pump, reactor, spectroscopic cell, injection/sampling block, transfer line, and two-way and three-way valves, was ca. 5.0 mL. The completed system was tested under vacuum as well as under pressure ($P_T = 8.0$ MPa).

The system was characterized in the absence of reaction with respect to gas–liquid mass transfer for the stirred tank, as well as mixing and recycle residence time distribution in the entire system. The system was also characterized in the presence of reaction, to confirm negligible liquid–solid transport resistance, negligible intraparticle diffusion resistance, and differential conversion over the packed bed.

4.1. System characterization in the absence of reaction: gas–liquid mass transfer and mixing and recycle residence time distribution

4.1.1. Gas–liquid mass transfer for the stirred tank

The overall mass transfer coefficients, $K_L a$, for hydrogen into toluene were determined in the 25-mL stirred tank (∅25 × 50 mm) at various stirring speeds using a magnetic stirring bar (∅9 × 15 mm). The range of stirring speeds covered in this study was 400–700 rpm.

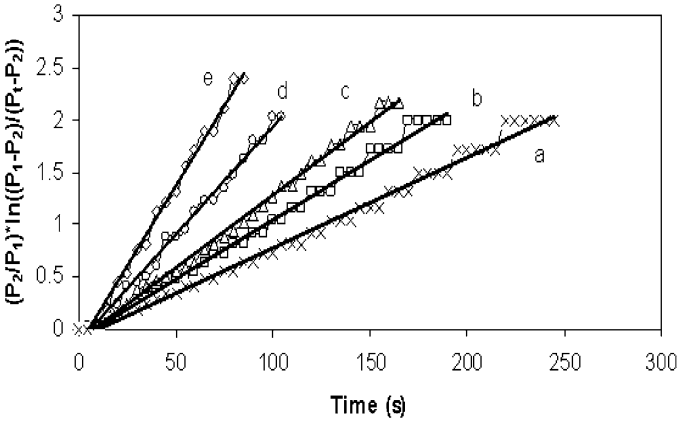

Fig. 6. The effect of stirring speeds on gas-liquid mass transfer in the 25 mL stainless stirred tank. The mass transfer coefficients (slopes) are: (a) 0.0086/s (300 rpm), (b) 0.0114/s (400 rpm), (c) 0.0139/s (500 rpm), (d) 0.0205/s (600 rpm), and (e) 0.0306/s (700 rpm).

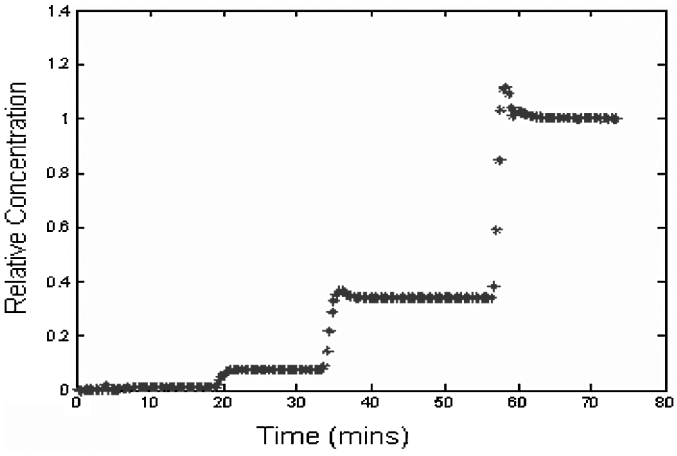

Fig. 7. The relative concentration profile of *d*-toluene obtained by injecting 2, 20, 100, and 250 µL into toluene at times 4, 17, 31, and 54 min.

The dynamic method of gas absorption was used to measure $K_L a$. This technique involves gas absorption into the liquid phase, resulting in decreased pressure of the enclosed gas phase [32,33]. The pressure decrease is then used to determine $K_L a$. The equation for calculating $K_L a$ from the time-dependent pressure decrease is

$$\frac{P_2}{P_1}\ln\left(\frac{P_1 - P_2}{P - P_2}\right) = K_L a \cdot t. \quad (1)$$

Hydrogen gas (99.99%, Soxal, Singapore) and toluene (99.9%, Mallinckrodt) were used for the experiment. A piezo-resistant pressure transmitter (PAA 27 W; range, 2.000 ± 0.001 bar absolute) connected to a digital LED indicator (Keller EV-94) were used to measure the absolute system pressure. Rotational speeds of the magnetic stirring bar were determined using a stroboscope (Nova-Strobe DA Digital AC, 30–14,000 fpm; Million Agencies). The stirrer speed settings of the high-field intensity Variomag magnetic stirrer and the stroboscopically measured speeds were consistent in the 400–700 rpm range, despite the 5-mm-thick stainless steel base plate.

The stirred tank was isolated for mass transfer experiments. A total of 10 mL of anhydrous toluene was transferred into the stirred tank and briefly vacuumed under stirring to remove any residual O_2/N_2 present. This provided a liquid level corresponding to an H/D of ca. 1. Hydrogen was then introduced into the head space above the toluene without stirring. After the initial pressure, P_1, was recorded, the stirrer was started and the decrease in pressure with time was measured. The final pressure, P_2, was noted when the pressure within the tank no longer decreased. Five mass transfer experiments were conducted by varying stirring speeds, and the relationship between $K_L a$ and stirring speed was determined. Fig. 6 shows the effect of stirring speed on gas–liquid mass transfer in the 25-mL stainless stirred tank. In this figure, the right side of the gas uptake function was evaluated and plotted versus time. The experimental data provided very reasonable straight lines, confirming the validity of using Eq. (1).

Ordinate values of 2 correspond to ca. 98% of the saturated dissolved gas liquid-phase concentrations. Accordingly, Fig. 6 indicates that the time required for saturation of the liquid phase was ca. 200 s at a stirring speed of 400 rpm. This time to saturation was deemed reasonable, and thus a stirring speed of 400 rpm was selected to avoid vortex problems. Previous open stirred tank experiments had shown that deep vortex formation occurred at ca. 600 rpm in the unbaffled tank.

4.1.2. Mixing and recycle residence time distribution in the entire system

Breakthrough tracer experiments were conducted by injecting different volumes of *d*-toluene (2, 20, 100, and 250 µL) into the system via the HPLC injection valves. D_8-toluene was selected as a tracer to avoid the problems caused by different physical properties of the solvent and solute. The entire system, as shown in Fig. 1, was filled with 15 mL of anhydrous toluene. The stirring speed was set at 400 rpm, and the pump was set to a flow rate of 2 mL/min. The relative concentration of d_8-toluene was determined by FTIR spectroscopy as a function of time and the results are given in Fig. 7.

Fig. 7 clearly shows that the tracer injections resulted in rapid and relatively sharp breakthrough curves. The typical time interval between an injection and the middle of a breakthrough curve was ca. 1.5 min in these experiments involving a 2-mL/min flow rate. The breakthrough curves demonstrate the typical overshoot that should be observed in tracer experiments conducted in closed systems with recycling that can be approximated by CSTR and PFR in series [34]. None of the data suggest the presence of dead volumes in the system or any other unusual mixing behavior.

4.2. System characterization in the presence of reaction: mass transfer and intraparticle diffusion test

4.2.1. Liquid–solid mass transfer

The issue of liquid–solid mass transfer was addressed by varying the LHSV—in other words, by varying the volumetric flow rate of the metering pump. A series of experiments was conducted under the standard reaction conditions with five different circulation flow rates, 3–7 mL/min. Standard conditions were as follows: catalyst loading, ca. 0.019 g; hydrogen

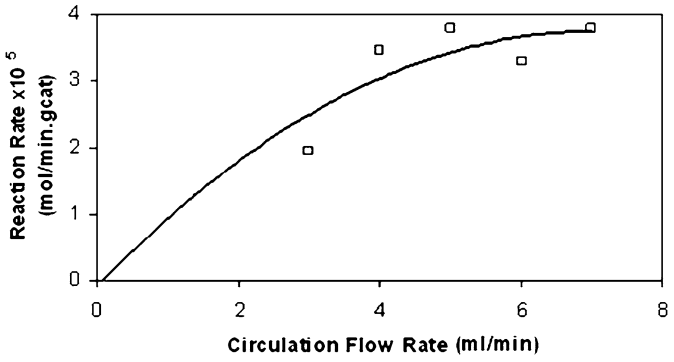

Fig. 8. Reaction rates based on the conversion of acetophenone over Pt/Al_2O_3 at 0 °C at different circulation flow rates.

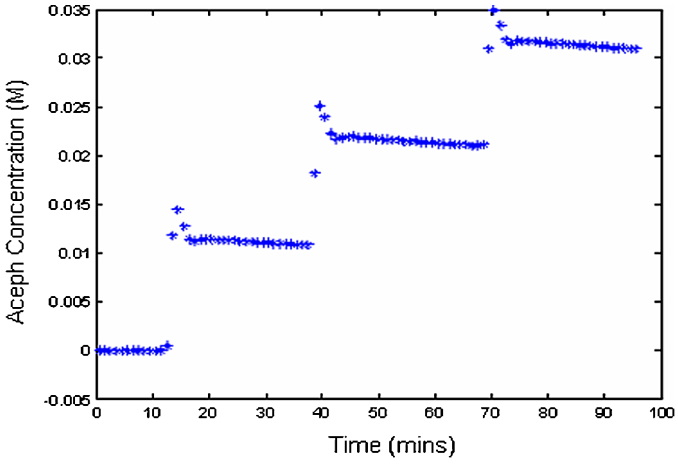

Fig. 9. The concentrations of the acetophenone vs. time after three different acetophenone perturbations at times 10, 35, and 64 min.

pressure, 1.75 bar; solvent toluene volume, 15 mL; and stirring speed, 400 rpm. At time $t = 0$ min, a program was executed to record the spectra every minute. At $t = 10$ min, 60 µL of acetophenone was injected through one of the HPLC six-port valves. Reaction rates based on the conversion of acetophenone are plotted in Fig. 8.

Fig. 8 indicates that reaction rate was dependent on the flow rate up to ca. 4 mL/min. Above a 4-mL/min flow rate, the reaction rates were almost constant. This indicates that liquid–solid mass transfer resistance is negligible at the higher flow rates used. Thus, a high flow rate (5 mL/min) was used in all subsequent parts of this catalytic study.

4.2.2. Intraparticle diffusion resistance

The Madon–Boudart criterion was used to address the issue of intraparticle diffusion resistance in a simple and straightforward manner. This approach avoids the detailed considerations involved in using the Thiele module. The catalyst Engelhard 4759 was sieved into three fractions: which included particle size >75 µm, particle size 75–53 µm, and particle size 53–45 µm. Different catalyst particle sizes were tested under otherwise similar standard reaction conditions. The texture parameters of various fractions of Engelhard 4759 have been determined elsewhere [33]. The turnover frequency (TOF) per Pt atom active site was used to calculate the activity of the catalyst. The TOFs of different fractions in the three particle size categories were ca. 0.007/s for >75 µm, 0.012/s for 53–75 µm, and 0.012/s for 45–53 µm.

The experimentally determined TOFs, using particle sizes 75–45 µm, were almost constant, indicating negligible intraparticle diffusion resistance. Accordingly, catalysts with particle size 45–75 µm were used for further experiments and multiple perturbations in this study. The primary reason for taking the center cut of the catalyst size distribution was to avoid the presence of too much fine material, which may accumulate at the 2.0-µm reactor frit and lead to excessive pressure drop.

4.2.3. Conversion per pass

Differential conversion per pass is an important criterion for good kinetic studies with packed beds. Usually, conversion of the reference component per pass <1% is considered differential. This leads to a situation in which all parts of the packed bed have a very similar composition. At the mean reaction conditions used in this study, the conversion of substrate per pass was ca. 0.25%, indicating that this reaction can be considered to occur at a nearly constant substrate concentration. The conversion of dissolved hydrogen per pass was ca. 3.5%.

4.3. Miscellaneous mass balance and mass transfer issues

The injection/sampling block introduces two interesting mass transfer-related issues. When injections occurred at time t with the six-way HPLC injection valves, x µL of reagent/solution was injected and x µL of system solution with composition C_t was removed. When samples were taken at time t with the six-way HPLC sampling valves, x µL of system solution with composition C_t was removed and x µL of pure solvent was introduced. The total mass balance for the system can be rigorously updated after each injection/sampling if necessary.

In principle, some liquid-phase solutes components may adsorb strongly on available surfaces (i.e., pump materials, circulation tubing and sealing materials, stainless steel components and optical windows). No evidence of this was found with the solutes used in the present study, however.

5. Multiple perturbations during reaction

As mentioned earlier, multiple perturbations can be useful for various reasons, and this can be used to demonstrate, at least in part, the utility of the present experimental apparatus/setup. As an illustration of this principle, a semibatch experiment was conducted in which three injections of 20-µL acetophenone were introduced through the injection valves. All of the remaining reaction conditions were consistent with the standard conditions used throughout this study. The concentrations of the reagent versus time are plotted in Fig. 9.

The reaction rates at three different reagent concentrations were 2.6×10^{-5} mol/(min g_{cat}) (0.011 M), 3.0×10^{-5} mol/(min g_{cat}) (0.021 M), and 3.0×10^{-5} mol/(min g_{cat}) (0.031 M). It is readily apparent that at low acetophenone concentrations, the rate increased with increasing acetophenone concentration,

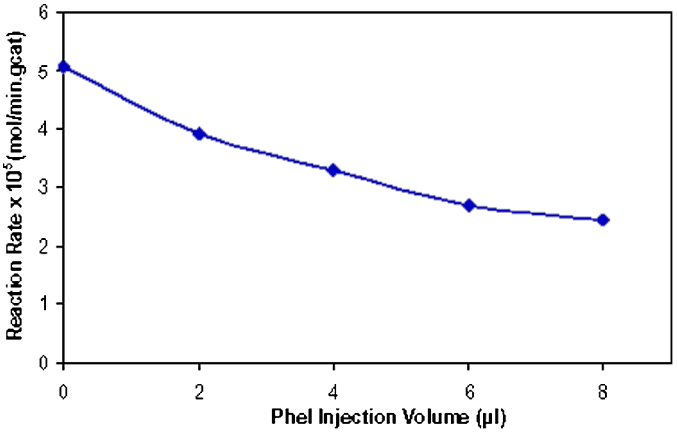

Fig. 10. Reaction rates for the conversion of acetophenone as a function of 1-phenylethanol injection volumes (obtained from different 1-phenylethanol perturbations in one semi-batch reaction).

whereas at high concentrations, the rate was almost independent of acetophenone concentration.

In a similar manner and in an independent experiment, 60 µL of acetophenone was injected into the reaction system at time $t = 10$ min, followed by injection of four perturbations of 1-phenylethanol in 2 µL volumes into the reaction system. The reaction rates at different product injection volumes from one semibatch experiment are plotted in Fig. 10. This figure clearly shows that the rates of reaction decreased with increasing product injection volumes.

6. Discussion and conclusion

The present study involves a compact experimental setup that facilitates exploratory and kinetic in situ/on-line spectroscopic studies of catalytic systems. Details of the construction have been provided, and the experimental setup has been characterized with respect to mass transfer. The setup exhibits quite reasonable mass transfer characteristics for slow to moderately rapid reactions (characteristic times on the order of 30 min or more). Although the catalytic test reaction reported here was heterogeneous in nature, a similar configuration can and has been used for homogeneous catalytic studies by our group.

In Section 1 we alluded to a number of related issues. One important issue is cost-effectiveness. Indeed, the in-house-designed components of our setup can be readily machined by most machine shops at a small fraction of the cost of commercial spectroscopic cells and commercial reactors. The injection/sampling block also can be readily constructed using commercial HPLC valves. The setup's cost-effectiveness provides considerable laboratory flexibility. For example, in our laboratories, platinum, iridium, rhodium, and palladium are all currently being used, and dedicated setups are reserved for each type of catalytic system, which helps prevent cross-contamination in experiments.

The addition of an easy-to-use injection block greatly facilitates experimental work. For example, batch experiments are readily converted to semibatch experiments in which a very wide range of reaction conditions can be spanned/surveyed in a short period. The ability to cover a wide range of reaction conditions with the least logistical/resource requirements significantly changes the way in which the investigation is carried out. This, of course, directly impacts the design of experiments, but the true utility derives from the implications for SMCR.

The combined use of multiple perturbations during heterogeneous catalysis and subsequent SMCR analysis appears to be quite novel. Indeed, this combination is probably nonobvious even for the majority of specialists in reaction engineering and catalysis. It provides a considerable departure from the conventional approach to conducting liquid-phase catalytic experiments, namely setting the initial condition and letting the batch go to completion. In the present approach, semibatch operation with a large number of perturbations greatly facilitates spectral deconvolution and further analysis.

The small displacements and volumes involved, together with the injection/sampling block, greatly facilitate isotopic labeling and even multiple simultaneous isotopic labeling experiments. In a simple example, one can consider the entire replacement of a normal hydrocarbon solvent with pure per-deuterated solvent. This immediately allows the accurate quantification of common ligands, reagents, and products, because the C–H spectral region is no longer saturated. In a more complex example, labeled or multiply labeled reagents can be readily used, because the amounts involved are modest (i.e., in the range of 10's of mg).

In summary, the present contribution has attempted to document a general and robust setup applicable to a wide range of common liquid-phase catalytic systems used in the catalytic community. As mentioned, our group is currently using this general setup to study a number of catalytic systems and detailed spectroscopic and kinetic analyses will be forthcoming.

Acknowledgments

This study was supported by grants from the Academic Research Fund of NUS. Research scholarships for F.G., K.I.K., and A.D.A. provided by the Graduate School of Engineering at the National University of Singapore are gratefully acknowledged. A postdoctoral fellowship for C.L.Z. from the Singapore Millennium Foundation is also gratefully acknowledged.

Supplementary material

CAD drawings, photographs and further information are included on 31 supplementary pages. The 25-mL stirred tank CAD drawing is easily modifiable as was done for our similar 50 and 100 mL volume stirred tanks. The 15 × 40 mm (thickness × diameter) cell CAD drawing is easily modifiable as was done to accommodate our similar 30 × 40 mm (thickness × diameter) KRS5 windows for high-pressure far infrared spectroscopy.

Please visit DOI:10.1016/j.jcat.2005.09.031.

References

[1] L. Damoense, M. Datt, M. Green, C. Steenkamp, Coord. Chem. Rev. 248 (2004) 2393.

[2] B. Heaton (Ed.), Mechanisms in Homogeneous Catalysis: A Spectroscopic Approach, Wiley–VCH, New York, 2005.
[3] W. Li, G.D. Meitzner, R.W. Borry, E. Iglesia, J. Catal. 191 (2000) 373.
[4] R.W. Borry, Y.-H. Kim, A. Huffsmith, J.A. Reimer, E. Iglesia, J. Phys. Chem. 103 (1999) 5787.
[5] T.E. Cranshaw, B.W. Dale, G.O. Longworth, C.E. Johnson, Mössbauer Spectroscopy and Its Applications, Cambridge Univ. Press, Cambridge, 1985.
[6] A. Drochner, M. Fehlings, K. Krauss, H. Vogel, Chem. Eng. Technol. 23 (4) (2000) 4.
[7] K. Almusaiteer, R. Krishnamurthy, S.S.C. Chuang, Catal. Today 55 (3) (2000) 291.
[8] T. Okuhara, Y. Hasada, M. Misono, Catal. Today 35 (1–2) (1997) 83.
[9] C. Li, P.C. Stair, Stud. Surf. Sci. Catal. A 105 (1997) 599.
[10] Z.L. Wu, H.S. Kim, P.C. Stair, S. Rugmini, S.D. Jackson, J. Phys. Chem. B 109 (7) (2005) 2793.
[11] T. Xu, J.F. Haw, J. Am. Chem. Soc. 116 (17) (1994) 7753.
[12] J.B. Butt, H. Bliss, C.A. Walker, AIChE J. 8 (1962) 42.
[13] G.E.P. Box, W.G. Hunter, J.S. Hunter, Statistics for Experimenters: An Introduction to Design, Data Analysis, and Model Building, Wiley, New York, 1978, p. 24.
[14] C.Z. Li, E. Widjaja, W. Chew, M. Garland, Angew. Chem. Int. Ed. 41 (20) (2002) 3786.
[15] W. Chew, E. Widjaja, M. Garland, Organometallics 21 (9) (2002) 1982.
[16] E. Widjaja, C.Z. Li, M. Garland, Organometallics 21 (9) (2002) 1991.
[17] C.Z. Li, E. Widjaja, M. Garland, J. Catal. 213 (2) (2003) 126.
[18] E. Widjaja, C.Z. Li, M. Garland, J. Catal. 223 (2) (2004) 278.
[19] C.Z. Li, E. Widjaja, M. Garland, J. Am. Chem. Soc. 125 (18) (2003) 5540.
[20] A.N. Collins, G.N. Sheldrake, J. Crosby (Eds.), Chirality in Industry: The Commercial Manufacture and Applications of Optically Active Compounds, Wiley, New York, 1995.
[21] Y. Orito, S. Imai, S. Niwa, J. Chem. Soc. Jpn. (1979) 1118;
Y. Orito, S. Imai, S. Niwa, J. Chem. Soc. Jpn. (1980) 670;
Y. Orito, S. Imai, S. Niwa, J. Chem. Soc. Jpn. (1982) 137.
[22] G. Webb, P.B. Wells, Catal. Today 12 (1992) 319.
[23] H.U. Blaser, H.P. Jalett, D.M. Monti, A. Baiker, J.T. Wehrli, in: Structure–Activity and Selectivity Relationships in Heterogeneous Catalysis, Elsevier Science Publishers B.V., Amsterdam, 1991, p. 147.
[24] A. Baiker, J. Mol. Catal. A 115 (1997) 473.
[25] M. Garland, H.U. Blaser, J. Am. Chem. Soc. 112 (1990) 7048.
[26] H.U. Blaser, M. Garland, H.P. Jalett, J. Catal. 144 (1993) 569.
[27] H.U. Blaser, H.P. Jalett, M. Garland, M. Studer, H. Thies, A. Wirth-Tijani, J. Catal. 173 (1998) 282.
[28] L. Chen, Y.J. Zhao, F. Gao, M. Garland, Appl. Spectrosc. 57 (7) (2003) 797.
[29] E. Brunner, J. Chem. Eng. Data 30 (1985) 269.
[30] L. Chen, M. Garland, Appl. Spectrosc. 56 (11) (2002) 1422.
[31] W.L. McCabe, J.C. Smith, P. Harriot, Unit Operations of Chemical Engineering, sixth ed., McGraw-Hill, New York, 2001.
[32] A. Deimling, B.M. Karandikar, Y.T. Shah, Chem. Eng. J. 29 (1984) 127.
[33] M. Garland, H.P. Jalett, H.U. Blaser, in: Heterogeneous Catalysis and Fine Chemicals, vol. II, Elsevier Science Publishers B.V., Amsterdam, 1991, p. 177.
[34] D.W.T. Rippin, Ind. Eng. Chem. 6 (1967) 488.